Environmental Science & Technology

Article

pubs.acs.org/est

Earthworms and Humans in Vitro: Characterizing Evolutionarily Conserved Stress and Immune Responses to Silver Nanoparticles

Yuya Hayashi,[†,‡,*] Péter Engelmann,[§] Rasmus Foldbjerg,[⊥] Mariann Szabó,[§] Ildikó Somogyi,[∥] Edit Pollák,[∥] László Molnár,[∥] Herman Autrup,[⊥] Duncan S. Sutherland,[†] Janeck Scott-Fordsmand,[‡] and Lars-Henrik Heckmann[‡]

[†]iNANO Interdisciplinary Nanoscience Center, Aarhus University, Ny Munkegade 120, 8000 Aarhus, Denmark

[‡]Department of Bioscience, Aarhus University, Vejlsøvej 25, 8600 Silkeborg, Denmark

[§]Department of Immunology and Biotechnology, Clinical Center, University of Pécs, Szigeti u. 12, Pécs H-7643, Hungary

[∥]Department of General Zoology, University of Pécs, Ifjúság u. 6, Pécs H-7624, Hungary

[⊥]Department of Public Health, Aarhus University, Bartholins Allé 2, 8000 Aarhus, Denmark

Supporting Information

ABSTRACT: Little is known about the potential threats of silver nanoparticles (AgNPs) to ecosystem health, with no detailed report existing on the stress and immune responses of soil invertebrates. Here we use earthworm primary cells, cross-referencing to human cell cultures with a particular emphasis on the conserved biological processes, and provide the first in vitro analysis of molecular and cellular toxicity mechanisms in the earthworm *Eisenia fetida* exposed to AgNPs (83 ± 22 nm). While we observed a clear difference in cytotoxicity of dissolved silver salt on earthworm coelomocytes and human cells (THP-1 cells, differentiated THP-1 cells and peripheral blood mononuclear cells), the coelomocytes and differentiated (macrophage-like) THP-1 cells showed a similar response to AgNPs. Intracellular accumulation of AgNPs in the coelomocytes, predominantly in a phagocytic population, was evident by several methods including transmission electron microscopy. Molecular signatures of oxidative stress and selected biomarker genes probed in a time-resolved manner suggest early regulation of oxidative stress genes and subsequent alteration of immune signaling processes following the onset of AgNP exposure in the coelomocytes and THP-1 cells. Our findings provide mechanistic clues on cellular innate immunity toward AgNPs that is likely to be evolutionarily conserved across the animal kingdom.

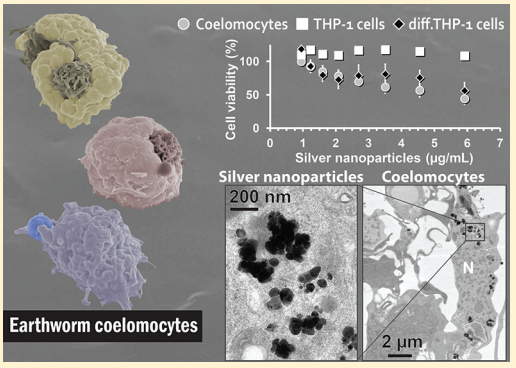

INTRODUCTION

Silver nanoparticles (AgNPs) are among the most widely commercialized nanomaterials. Environmental implication of daily use of nanosilver products is emerging; for example, the release of AgNPs and/or their derivative form (Ag^+) in washwater of commercial textile nanoproducts.[1] The recent discovery of silver sulfide nanocrystals in the sewage sludge materials[2] indicates that soil amendment process may in fact deliver AgNPs (as discharged or crystallized from complexation of Ag^+ and/or direct oxysulfidation)[3] to the terrestrial environment. Much less is known, however, about the potential impacts of nanosilver materials on the soil ecosystem health, with limited publications using earthworms as indicator soil organisms (e.g., bioavailability,[4] effects on the life-history traits,[5,6] apoptotic response,[7] and avoidance behavior[8]). Exposure of organisms in the soil matrices, which are often complex and heterogeneous, renders physicochemical in situ characterization of NPs challenging, and the mechanistic understanding of how AgNPs may disrupt the organism's physiology remains unclear. This is in contrast to in vitro models which benefit from the ease of controlling exposure conditions. In vitro models create a platform for a targeted approach to study the molecular and cellular basis of toxicity mechanisms, although the nanomaterials may undergo considerable transformation throughout the environmental/biological matrices[3] before reaching the target organ(s) of the test organism.

Invertebrate models, in comparison to vertebrate counterparts, have been used to study the evolutionary aspects of fundamental biological processes,[9] in which earthworms provide a model of precursory innate immunity expressing, for example, opsonization and phagocytosis.[10] Central in the earthworm's immunity against environmental pathogens and toxicants are the free-circulating immune cells, collectively called coelomocytes, in the coelomic fluid. Functioning as the first line of active defense, coelomocytes are presumably endowed with the ability not only to maintain the bacterial

Received: January 9, 2012
Revised: March 9, 2012
Accepted: March 12, 2012
Published: March 20, 2012

   dx.doi.org/10.1021/es3000905 | Environ. Sci. Technol. 2012, 46, 4166–4173

balance of the host but also to detoxify metals (e.g., compartmentalization and trafficking of cadmium[11]). Those functional characteristics led us to compare earthworm coelomocytes with human leukocytes that share similar immunobiology (e.g., clearance of particles/pathogens and metal homeostasis).

The aim of this study was to explore the mode of cytotoxicity of AgNPs and the soluble Ag^+ (silver nitrate; $AgNO_3$) by examining differences in the cell types affected, and to compare the effects of AgNPs on oxidative profile and expression patterns of selected biomarker genes that are highly conserved between the earthworm *Eisenia fetida* and humans. To facilitate dispersion of AgNPs in serum-supplemented cell culture media, we employed an albumin pretreatment procedure (see methods in ref 12) and characterized the AgNPs under exposure conditions. Cytotoxicity concentration−response correlations were established for earthworm coelomocytes and for human monocytes with or without differentiation into a macrophage-like phenotype. Silver accumulation in those cells was studied to investigate whether there is a correlation to cytotoxicity. Molecular analysis was made of the coelomocytes and human monocytes exposed to AgNPs, where oxidative stress profile, determined as the intracellular reactive oxygen species (ROS) level, and gene expression patterns were compared at early exposure time points (up to 6 h). Our results suggest important involvement of phagocytes, an evolutionarily conserved immune effector cell-type, in the toxicity mechanisms of AgNPs.

EXPERIMENTAL SECTION

Materials. Spherical AgNP powder (99.9% purity, capped with 0.2 wt %/wt polyvinyl pyrrolidone) was purchased from NanoAmor (Houston, TX). A colloidal suspension of the AgNP powder was prepared (see Supporting Information (SI) for details) and immediately mixed with a freshly prepared bovine serum albumin (BSA; Sigma-Aldrich) solution at 1:1 mass ratio. Within the AgNP concentration range used for the in vitro assays (described below), this amount of BSA contributes <1% of serum mass supplemented. The total silver concentration was determined by flame atomic absorption spectrophotometry (F-AAS). The endotoxin level was 0.801 EU/mL. Detailed methods of F-AAS and endotoxin tests are described in the SI. Dissolved $AgNO_3$ was purchased from Sigma-Aldrich and used as provided. The concentration of $AgNO_3$ was calculated on the molecular weight of silver and expressed as Ag^+.

Particle Characterization. The primary size and morphology of AgNPs were assessed under a transmission electron microscope (TEM) followed by image analysis to establish particle size distributions. Dynamic light scattering (DLS) was used to estimate the hydrodynamic size of AgNPs in Milli-Q water and in cell culture media (described below) with or without 1% heat-inactivated fetal bovine serum (FBS; HyClone). DLS analysis was performed within 1 h after preparation and after 24 h incubation at room temperature (RT) or 37 °C to investigate the colloidal stability. Zeta potential measurements were conducted on AgNPs after 24 h incubation at RT or 37 °C in cell culture media with or without 1% FBS to observe the shift in the potential upon association of AgNPs with serum proteins following a method described by Casals and co-workers.[13] Details of the particle characterization methods are described in the SI.

Soluble Silver Fraction. Soluble silver fraction of AgNPs under exposure conditions was investigated using an ultracentrifugation method[14] followed by graphite furnace AAS (GFAAS) analysis of total Ag. A concentration series of AgNPs (0.75−6.00 μg Ag/mL) was incubated for 24 h at RT or 37 °C in Milli-Q water or in cell culture media containing 1% FBS. Subsequently, AgNPs were ultracentrifuged at 100 000−150 000*g* and the supernatant was used for the analysis of total Ag concentration (see SI for details).

Cell Cultures. We used earthworm coelomocytes (primary cells), THP-1 cells (a human acute monocytic leukemia cell line) and their differentiated, macrophage-like phenotype (hereafter "diff.THP-1 cells") in this study. Adult *Eisenia fetida* (Oligochaeta, Lumbricidae) were obtained from ECT Oekotoxikologie GmbH (Flörsheim, Germany), and depurated for 1−2 days on filter paper moistened with deionized water. Coelomocytes were then harvested prior to each assay following the method previously described[15] (see SI for details). THP-1 cells were obtained from the German Collection of Microorganisms and Cell Cultures (DSMZ, ACC 16). Diff.THP-1 cells were prepared following the method of Park and others[16] by incubating THP-1 cells with 5 ng/mL phorbol 12-myristate 13-acetate (PMA; Sigma-Aldrich) for 48 h under the culturing condition. Differentiation of THP-1 cells was visually inspected and verified under an inverted light microscope. All cell types were cultured in RPMI-1640 medium (Invitrogen) supplemented with 2 mM l alanyl-L-glutamine (Invitrogen), 1% penicillin-streptomycin (Invitrogen) and 1−10% heat-inactivated FBS (hereafter referred to as RPMI/x%FBS). In all cases, the number of viable cells was determined by trypan-blue dye-exclusion and each assay was performed at a cell density of $2-3 \times 10^5$ cells/mL. Coelomocytes were maintained at RT while THP-1 cells were kept in a humidified atmosphere at 37 °C and 5% carbon dioxide during the course of each assay.

Human Peripheral Blood Mononuclear Cells. As primary cells are generally considered to be more vulnerable than cultured cancer cell lines, a supplemental study for Ag^+ cytotoxicity was conducted with human peripheral blood mononuclear cells (PBMCs) obtained from fresh blood of healthy individuals (n = 10, 5 female and 5 male blood donors) by Ficoll (Amersham Pharmacia Biotech Europe, Sweden) gradient centrifugation following the standard protocol. The PBMC layer was removed and washed in RPMI-1640 medium supplemented with 1% penicillin-streptomycin (Lonza, Switzerland) and 1% heat-inactivated FBS (Invitrogen). Studies were approved by the Regional Research Ethics Committee of the Faculty of Medicine at the University of Pécs (3796/2010) and written consent forms were obtained from all the blood donors.

Cytotoxicity Assay. Cytotoxicity was assessed using a cell counting kit-8 (Probior, Germany) that employs a water-soluble tetrazolium salt (WST-8). The assays were conducted for coelomocytes, THP-1 cells and diff.THP-1 cells in RPMI/1%FBS following the manufacturer's protocol. The exposure concentrations were chosen according to our previous study on THP-1 cells[17] and ranged 0−1.35 μg Ag/mL (Ag^+) and 0−5.91 μg Ag/mL (AgNP). Absorbance at 450 nm (reference at 650 nm) was measured on a microplate reader (EL800, Bio-Tek Instruments, Denmark) after 24 h exposure (including 2 h incubation with WST-8). No interference of AgNPs was observed in the measured absorbance at the highest concentration used in this study. As a supplemental study,

dx.doi.org/10.1021/es3000905 | Environ. Sci. Technol. 2012, 46, 4166−4173

Table 1. List of Target Genes Selected Based on the Biological Functions and BLAST Search[a]

representative biological process	*Eisenia fetida* coelomocytes	*Homo sapiens* THP-1 cells	sequence similarity	
			identity/positives	*E*-value
stress signal transduction	MEK kinase 1 (MEKK1)	MEK kinase 1 (MEKK1)	37%/55%	1×10^{-25}
cellular functions	protein kinase C1 (PKC1)	protein kinase C epsilon (PRKCE)	82%/91%	1×10^{-57}
innate immune systems	myeloid differentiation factor 88 (MyD88)	myeloid differentiation factor 88 (MyD88)	50%/63%	6×10^{-13}
general stress responses	heat shock 70 kDa protein (HSP70)	heat shock 70 kDa protein 8 (HSPA8)	90%/98%	1×10^{-64}
metal detoxification	cadmium−metallothionein (MT)	metallothionein 2A (MT2A)	38%/58%	9×10^{-1}
antioxidizing mechanisms	catalase (Cat)	catalase (Cat)	74%/84%	7×10^{-62}

[a]Representative biological processes of genes were annotated based on the bioinformatic databases Gene Ontology (GO) and Kyoto Encyclopedia of Genes and Genomes (KEGG).

the same assay was performed for each set of PBMCs from different individuals (Ag^+ treatment only).

Cellular Accumulation of AgNPs. Based on the concentration−response curves established in the cytotoxicity assay, coelomocytes, THP-1 cells and diff.THP-1 cells (total 8 × 10^5 cells each) were exposed to low (Ag^+: 0.05 μg/mL, AgNP: 2 μg/mL) or moderate (Ag^+: 0.1 μg/mL, AgNP: 4 μg/mL) silver concentration for 24 h. Unexposed cells were included as negative controls. Cell-free background samples (for each silver treatment) were included to take into account sedimentation of AgNPs during centrifugal isolation of cells (300*g*, 5 min). After exposure, the cells were washed twice in phosphate buffered saline (PBS). Small aliquots of each cell suspension were stained with trypan-blue and examined using an automated cell counter (Countess, Invitrogen). Remaining cells were pelleted and digested in 69% HNO_3. Total Ag was quantified by GFAAS as described in the SI (see the detailed method for soluble silver fraction measurements), and data from each treatment was subtracted with the corresponding cell-free background value and normalized by the number of cells. Ultrathin sections of coelomocytes after a 24 h exposure to AgNPs (2.32 μg/mL) were examined under a TEM to verify the uptake and intracellular localization of AgNPs (see SI for details). Side scatter analysis was performed as a part of flow cytometric ROS assay (see below).

ROS Assay. The intracellular ROS profile of AgNP-treated coelomocytes and THP-1 cells was studied in a time-resolved manner. The fluorescent marker 2′,7′-dichlorodihydrofluorescein diacetate (H_2DCF-DA; Sigma-Aldrich) was used following a recommended procedure[18] and in combination with 7-aminoactinomycin D (7-AAD; Sigma-Aldrich) staining as a marker for membrane damages. Briefly, cells were exposed to AgNPs (5.91 μg/mL) or the ROS inducer t-butyl hydroperoxide (TBHP; Sigma-Aldrich, 0.05 mM) in phenol red-free RPMI/1%FBS. Following 1, 3, or 6 h exposure, the cells were loaded with 10 μM H_2DCF-DA. After 30 min, the medium was changed and the cells were stained with 4 μg/mL 7-AAD and immediately analyzed by flow cytometry (Cell Lab Quanta SC MPL, Beckman Coulter). The 488 nm laser was used for excitation and DCF was detected in FL1 (525/30 BP filter), whereas 7-AAD was detected in FL3 (670 LP filter). Standard compensation was performed in the Quanta SC MPL Analysis software (Beckman Coulter) using unstained and singly stained cells. For each sample, a total of minimum 15 000 cells was gated for analysis in FlowJo 7.6.4 (Tree Star Inc., OR). In the coelomocyte samples, two major populations were isolated based on the physical parameters (amoebocytes and chloragocytes; see SI, Figure S1) and fluorescence from the amoebocyte population was studied (chloragocytes were excluded due to their strong autofluorescence). Mean DCF fluorescence of cells without membrane leakage of the dye (DCF+, 7-AAD−) was normalized to the unexposed control of the corresponding time point.

Gene Expression Pattern. To study the gene response patterns, coelomocytes and THP-1cells (total 1 × 10^6 cells each) exposed to AgNPs (as in the ROS assay) were subsequently mixed with RNAlater (Ambion) and stored at −80 °C. Detailed methods of total RNA extraction, cDNA synthesis and real-time quantitative polymerase chain reaction (qPCR) are described in the SI. The qPCR analysis was performed on six biomarker gene categories as molecular signatures of events relating to stress and immune responses to AgNPs. The selection of target gene ortholog pairs was based on their vital function within the representative biological process and the high degree of conservation (>50% sequence similarity) between *E. fetida* and humans as determined by basic local alignment search tool (BLAST) analyses (Table 1). The sequences of the analyzed genes were obtained from GenBank. Accession numbers and primer sequences are listed in SI Table S1. Each qPCR reaction contained 5 μL of cDNA template along with 900 nM primers in a final volume of 15 μL. Melting curves were visually inspected to verify a single amplification product with no primer-dimers. Each treatment/time point (0, 1, 3, and 6 h) was replicated four times.

Data Analysis. EC_x values were estimated using 2-parameter logistic regression ($Y = Y_0/(1 + e^{4s(X-X50)})$; logging exposure concentration) in TRAP statistics. One-way analysis of variance (ANOVA) was performed for difference between the cell types (Cytotoxicity assays) with Levene's test to test the equality of variances followed by Tukey's HSD test for a multiple comparison (Origin Pro 8, OriginLab, MA). Student's *t*-test was performed in Microsoft Excel. For all parametric tests, measurement values were log-transformed to satisfy the assumption of normal distribution and significance was determined as $\alpha = 0.05$. The raw qPCR data were analyzed with data analysis for real-time PCR (DART-PCR).[19] Gene expression was normalized with NORMA-Gene, a novel normalization approach based on a data-driven algorithm which does not require the use of reference genes.[20] Correspondence analysis (CA; multivariate analysis) was performed to identify correspondence between the gene response pattern and the exposure time points, using standardized data (Proc Corresp, SAS 9.1.3, SAS Institute Inc., NC).

RESULTS

Primary and in Situ Characterization of AgNPs. TEM imaging of AgNPs showed a normally distributed size frequency with a mean of 83 ± 22 nm (SD, $n = 587$) (SI, Figure S2). At the highest test concentration used in this study

(5.91 μg/mL) the calculated number of NPs was 2×10^9/mL and thus exposure of cells to AgNPs was $7-8 \times 10^3$ NPs/cell in each assay, assuming that the particle is spherical and monodispersed with a single size of 83 nm. From the particle size distribution, specific surface area was estimated as 6 m^2/g. DLS analysis revealed an average hydrodynamic size of 110 ± 51 nm (polydispersity index [*PdI*] = 0.218; z-average ± *PdI* width), but displaying a bimodal distribution (SI, Figure S2). The intensity peak at 20−30 nm corresponds to the size of free PVP measured separately (SI, Figure S2). Colloidal stability of AgNPs was tested in cell culture media with or without 1% FBS. There was no difference in the size distributions of AgNPs in Milli-Q water and in cell culture media without serum after 24 h incubation at RT or 37 °C, while the addition of serum (1% FBS) shifted the distribution toward larger sizes (SI, Figure S2). As anticipated from the DLS analysis, AgNPs after 24 h incubation in the presence of 1% FBS showed a shift of zeta potential values from ca. −14 mV (AgNPs incubated and resuspended in 0% FBS) to ca. −10 mV (AgNPs incubated in 1% FBS, resuspended in 0% FBS) (SI, Figure S3) probably a result of changes in hard-shell composition of the protein corona on NPs as reported by Casals and colleagues.[13] The soluble silver fraction (as measured by an ultracentrifugation method[14]) of AgNPs incubated for 24 h in Milli-Q water or RPMI/1%FBS (in vitro test medium) at RT or 37 °C was 2−8% (SI, Figure S4). The factors affecting the oxidative dissolution kinetics could not be resolved in this study, although there appears to be a general trend that a higher temperature and low AgNP concentrations may have a larger effect on the soluble silver fraction than the difference between distilled water and RPMI/1%FBS.

Cytotoxicity Comparison between Different Cell Types. WST-8 assays were performed to establish toxicity concentration−response curves for coelomocytes, THP-1 cells and diff.THP-1 cells exposed to Ag^+ or AgNPs for 24 h. Viability of coelomocytes decreased faster with increasing Ag^+ concentrations than the other cell types (Figure 1A and SI, Table S2). The same assay was also performed with human PBMCs and the concentration−response curve and corresponding EC_x values lay in the similar range to those of THP-1 cells and diff.THP-1 cells but not to those of coelomocytes (Figure 1A and SI, Table S2). Despite the differential sensitivity to Ag^+, coelomocytes and diff.THP-1 cells were affected alike at lower AgNP concentrations compared to THP-1 cells where EC_x values could not be estimated within the concentration range tested (Figure 1B and SI, Table S2). The fitted concentration−response curve functions on coelomocytes and diff.THP-1 cells varied between replicated assays compared to those fitted in the Ag^+ treatments (SI, Table S2). Furthermore, the smaller curve steepness, *S*, in the AgNP treatments shows the lower cell viability loss with increasing exposure concentration than in the Ag^+ treatments.

Cellular Accumulation of AgNPs. We used GFAAS to quantify cellular accumulation of silver species in coelomocytes, THP-1 cells and diff.THP-1 cells following a similar exposure setting as performed for the cytotoxicity assay. At the low concentration of AgNPs (2 μg/mL), coelomocytes accumulated silver significantly more than undifferentiated THP-1 cells (Figure 2A). Roughly estimated from the obtained silver concentrations, the numbers of AgNPs accumulated were in ranges of several 10^0-10^2 NPs/cell (THP-1 cells; 5 ng Ag/10^5 cells) and 10^1-10^3 NPs/cell (coelomocytes; 42 ng Ag/10^5 cells, and diff.THP-1 cells; 101 ng Ag/10^5 cells) depending on the

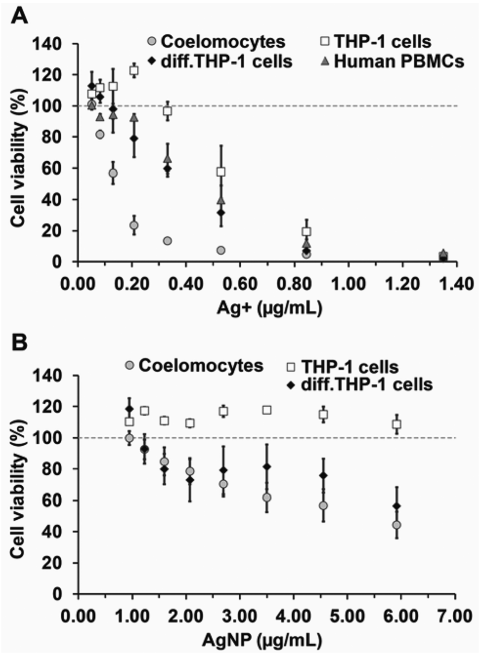

Figure 1. Cytotoxicity comparison between cell types following 24 h exposure to a concentration series of (A) Ag^+ and (B) AgNP. Circles: coelomocytes; Squares: THP-1 cells; Diamonds: diff.THP-1 cells; Triangles: human PBMCs (Ag^+ only). Cell viabilities are plotted as mean ± SE of three to five independent assays relative to the unexposed controls.

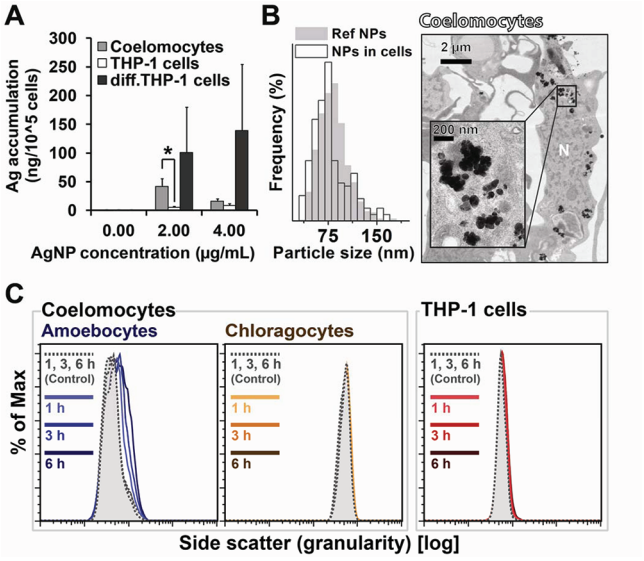

Figure 2. Cellular accumulation of AgNPs. (A) GFAAS analysis of cells after 24 h exposure to AgNPs. Values are mean ± SE of three independent assays. Asterisk denotes a significant difference (Student's *t*-test, $p < 0.05$). (B) TEM image depicting intracellular localization of AgNPs in coelomocytes after 24 h exposure to AgNPs (2.32 μg/mL). *N* = nucleus. Scale bars are 2 μm and 200 nm (close-up). EDS analysis verified the presence of Ag (SI, Figure S6). Size distribution of AgNPs found within the cells ("NPs in cells", $n = 227$) was comparable to the distribution of primary particle sizes ("Ref NPs", $n = 587$). (C) Time-course profile of side scatter increase in the two populations of coelomocytes and THP-1 cells exposed to AgNPs (5.91 μg/mL) for 1, 3, and 6 h. Cells with intact membranes (7-AAD negative) are shown for amoebocytes and THP-1 cells. The histograms display a representative of one of three independent assays.

dx.doi.org/10.1021/es3000905 | *Environ. Sci. Technol.* 2012, 46, 4166−4173

particle size (40−120 nm) and assuming all silver is in the form of a NP. At the moderate concentration (4 μg/mL), however, we observed less silver accumulation in coelomocytes, which could be due to membrane damages (83% viability, 7-AAD staining of amoebocytes, unpublished data) while THP-1 and diff.THP-1 cells remained rather intact (determined from trypan-blue exclusion). In general although we found a differential pattern of silver accumulation between Ag^+- and AgNP-treated cells (Figure 2A and SI, Figure S5), the GFAAS approach does not distinguish the chemical state of Ag and whether NPs are internalized or only adhered to the cell membranes. To verify the uptake of AgNPs, we examined coelomocytes under a TEM mounted with energy-dispersive X-ray spectroscopy (EDS) for elemental analysis, and observed accumulation of AgNPs in several different cellular compartments but not typically in the nucleus (Figure 2B and SI, Figure S6A). Notably, AgNPs were found mainly in amoebocytes while less is identified in a chloragocyte-enriched sample (SI, Figure S6B). Mean particle size of AgNPs found within the cells was 79 ± 35 nm (SD, n = 227) showing a comparable distribution to that obtained in the primary particle size analysis (83 ± 22 nm, SD, n = 587). Finally, flow cytometric analysis of light scatter, which has been suggested as a means of detecting cellular accumulation of NPs,[21] supported the preferential uptake of AgNPs by the amoebocyte population of coelomocytes during 1−6 h exposure (Figure 2C).

Intracellular ROS Profile. As an indicator of oxidative stress, we measured the cellular level of ROS in coelomocytes (amoebocytes) and THP-1 cells following 1−6 h exposure to AgNPs (5.91 μg/mL). In general, an immediate suppression was observed in THP-1 cells after 1 h, whereas the ROS level of amoebocytes gradually increased over time (Figure 3). Exposure of THP-1 cells to the ROS inducer TBHP (0.05 mM) showed an initial increase followed by a rapid decrease. This could be explained by instantaneous deployment of antioxidizing mechanisms. In contrast, AgNPs and TBHP induced ROS in amoebocytes in a similar manner (Figure 3).

Gene Expression Patterns. In parallel with the ROS assays, we used the same concentration of AgNPs (5.91 μg/mL) to gain molecular insights into the observed toxicity and related ROS levels. At this concentration, cell viability was not affected at any of time points investigated (1, 3, and 6 h; SI, Figure S7). The first two dimensions of CA plots explained 92% and 94% of the variation in the data sets for coelomocytes and THP-1 cells, respectively (Figure 4). The gene responses clearly corresponded to hours of exposure in coelomocytes and THP-1 cells, both displaying a primary association with the stress-related genes, *MEKK1*, *HSP70*, and *Cat* (Figure 4 and SI, Figure S8). Remarkably, while coelomocytes showed down-regulation of those genes at 3 h, THP-1 cells marked significant induction of *MEKK1* and *HSPA8* in concert with characteristic transcription (>7-fold increase) of the metallothionein-encoding gene *MT2A* (SI, Table S3). *PKC1/PRKCE*, a gene encoding a central signal transducer for cellular function, and immune-related gene (*MyD88*) were upregulated and seemingly corresponded to a later time point (6 h) in both coelomocytes and THP-1 cells (Figure 4 and SI, Table S3).

DISCUSSION

This study was aimed at characterizing the mode of action of AgNPs in immune cells using a controlled exposure setting. We showed here selective cytotoxicity and preferential uptake of AgNPs in coelomocytes and diff.THP-1 cells. Further, the early

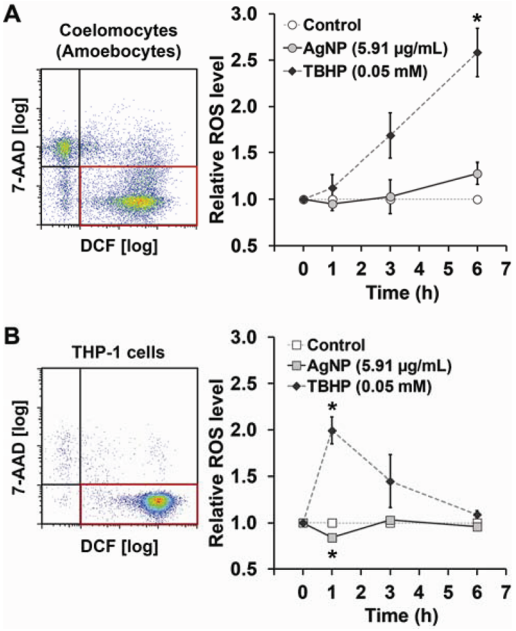

Figure 3. Time-course profiles of intracellular ROS level in (A) coelomocytes (amoebocytes) and (B) THP-1 cells. Cells were exposed to a fixed concentration of AgNPs (5.91 μg/mL) for 1, 3, and 6 h. Shown on the left are the quadrant regions gated for DCF/7AAD double-staining (representative, AgNP-treated cells at 1 h). DCF fluorescence of cells without membrane leakage (DCF+, 7AAD-; red gate) was recorded as the intracellular ROS level (right). Values are plotted as mean ± SE of three independent assays relative to unexposed controls of the corresponding time point. Solid line; AgNP treatment, Dashed line/Diamonds; TBHP treatment. Asterisks denote a significant difference between the treatment and the corresponding control population (Student's t-test, $p < 0.05$).

molecular responses to AgNPs involved an apparent transition from stress- to immune-related genes both in coelomocytes and THP-1 cells, but with a distinct induction of metallothionein-encoding gene in THP-1 cells.

Controlled exposure conditions are the strength of in vitro models, albeit still challenging with the introduction of NPs which creates complex solid−liquid interfaces at nanoscales. Encouraged by the dispersion method of Bihari and co-workers,[12] we pretreated AgNPs with BSA, one of the most abundant proteins in serum that is commonly used as a cell culture supplement. In fact, several proteomic studies have revealed that, through nonspecific adsorption, serum albumin is primarily the main constituent of the protein corona that is formed immediately after introduction of NPs to serum-supplemented culture media.[13,22] Pre-equilibration of AgNPs with BSA at low ionic strength ensures that the NPs are sterically protected at the transition from a low- to a high-ionic strength condition such as cell culture media. We demonstrated stable dispersion of AgNPs in cell culture media with and without serum. The same AgNPs without BSA pretreatment aggregated under the same condition or showed initial agglomeration even with the presence of serum (cf. SI Figure S2 compared to Figure 2 in ref 17). Further, because the NP-protein interaction is a dynamic process involving binding kinetics, when serum is added to the medium, adsorbed BSA can be exchanged or complexing with other serum proteins. This is indicated by increased hydrodynamic radius in DLS and reduced zeta potential of AgNPs after incubation in 1% FBS (and subsequent resuspension in the same media without

dx.doi.org/10.1021/es3000905 | Environ. Sci. Technol. 2012, 46, 4166−4173

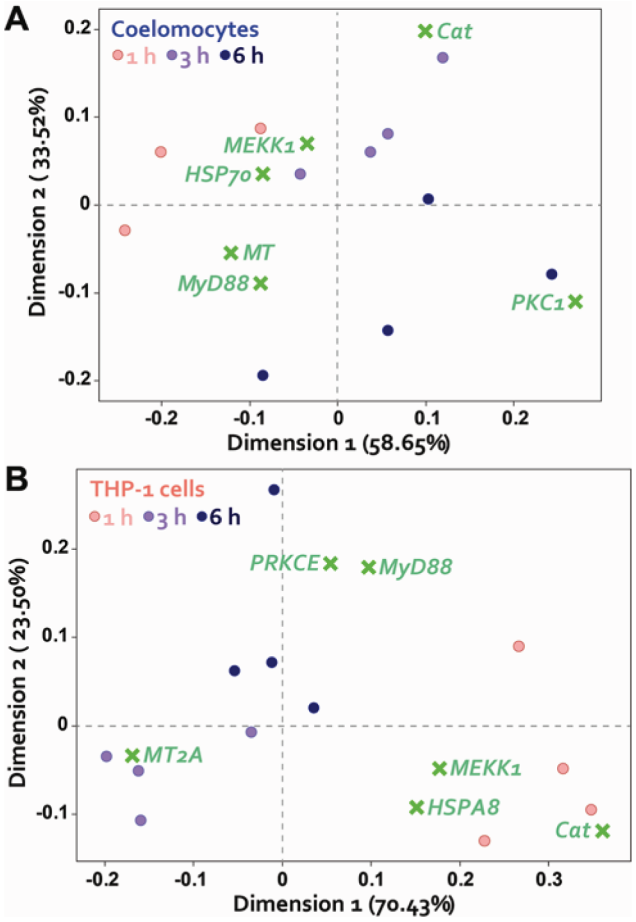

Figure 4. Correspondence analysis of gene expression data. Gene response patterns of (A) coelomocytes and (B) THP-1 cells following 1−6 h exposure to AgNPs (5.91 μg/mL). The first two dimensions are displayed (Crosses: gene, Dots: time of exposure). The distance between a dot (sample at the specified time of exposure) and each cross (gene) represents the relative importance of the changes in gene expression at the exposure time. Hence, dots in the proximity of a cross suggest an association between the exposure time and the gene.

serum), as these changes observed in this study illustrate the characteristics of NP-protein corona formation after serum exposure.[13,23] This suggests that, under the in vitro test conditions, AgNPs are likely to form a coexisting NP-protein assembly expressing altogether as a biologically relevant entity to be read by the cells.[23]

We assessed the cytotoxicity of Ag^+ and showed that the EC_{50} values lie in the concentration range previously determined for observable toxic effects to immunocytes.[24] Our results also show that there was a clear difference in sensitivity to Ag^+ between earthworm coelomocytes and the human leukocytes. A supplemental study on human PBMCs stressed that the coelomocytes are more susceptible even among primary cells. Despite the observed cell type-specific sensitivity differences to Ag^+, the AgNP cytotoxicity assay revealed diff.THP-1 cells having a strikingly similar concentration−response curve to that of coelomocytes. This shows an intriguing correlation with our finding that coelomocytes and diff.THP-1 cells accumulated more silver than undifferentiated THP-1 cells. Although the contribution of AgNP-derived Ag^+ could not be ruled out, the dissimilarity of the types of cells affected between the Ag^+- and AgNP-treatments is likely to be an indication of differential mode of toxicity specific to NPs. Preferential uptake of AgNPs by diff.THP-1 cells is not surprising because, in contrast to the precursor monocytic phenotype, these cells have an enhanced capability of NP internalization when serum proteins are present.[25] Of the identified coelomocyte populations, hyaline amoebocytes are proposed to be the putative evolutionary progenitor of mammalian monocytes and macrophages[10] and known to play a central role in clearance of particles by phagocytosis.[15] Indeed, our TEM investigation suggests intracellular localization of AgNPs predominantly in the amoebocyte population of coelomocytes. Size statistics of AgNPs found within the cells indicated that they originated from the AgNPs added and not products of biosynthesis from Ag^+ sources. A possibility exists, however, that the TEM sample preparation affected intracellular distribution and cell-surface adherence of AgNPs. More thorough studies would be needed to examine the uptake pathway (i.e., biologically driven) and how much of the AgNPs remain adhered to the cell membrane through physicochemical interactions.

Phagocytic uptake of AgNPs in return may explain the observed selective toxicity. For instance, intracellular accumulation of AgNPs could act as a source of Ag^+ mediating cellular damage in situ, a putative mechanism known as the "Trojan-horse effect" (*sensu* Limbach et al.[26]). Navarro and colleagues previously described that the calculated toxicity of AgNPs was higher than dissolved silver salt in algae when compared as a function of Ag^+ released.[27] Intracellular release of Ag^+ is plausible in the cellular environment, for example, at the low lysosomal pH (see ref 28 for the influence of pH on oxidative dissolution of AgNPs). Furthermore, not only via intracellular accumulation, but also when they encounter nonphagocytosable silver objects macrophages proved capable of forming a membrane at the interface within which the silver surface are oxidized releasing Ag^+ that is readily taken up by the cells.[29] We therefore emphasize that phagocytes, a fundamental unit of immune system, may play a considerable role as scavengers of AgNPs effecting cytokine release and even death of the cell.

The oxidative stress profile and expression patterns of evolutionarily conserved biomarker genes further illuminate a link to immune functions in response to the onset of AgNP exposure. Of the six gene categories studied, *MEKK1* (stress signal transduction), *HSP70/HSPA8* (general stress response) and *Cat* (antioxidizing mechanisms) were similarly regulated at early stages of the exposure (1−3 h), whereas *PKC1/PRKCE* (cellular functions) and *MyD88* (innate immune signaling) were more pronounced at a later time point (6 h). *MT/MT2A* (metal detoxification) was consistently expressed at high levels in THP-1 cells but not in coelomocytes. Metallothioneins, the translated products of *MT/MT2A*, are cysteine-rich proteins known to play a dual role as an early defense against toxic metal ions and oxidative stress.[30] As an early response to AgNPs of the same concentration, THP-1 cells were able to suppress (or even overwhelm) ROS generation (Figure 3) perhaps by fast deployment of antioxidizing mechanisms along with metallothioneins. The transcriptional evidence supports this view, whereby the stress-stimulated signal transduction via mitogen-activated protein kinases (MAPKs) (e.g., *MEKK1*) coordinates the protective proteins such as metallothioneins (MT/MT2A) and molecular chaperones (HSP70/HSPA8). The three genes were induced by AgNPs in THP-1 cells with a characteristic peak at 3 h in parallel. In support of this remark, AgNP-induced oxidative damage and MAPKs activation have been observed in

dx.doi.org/10.1021/es3000905 | *Environ. Sci. Technol.* 2012, 46, 4166−4173

human T lymphocytes[31] and murine fibroblasts.[32] Oxidative stress in *Drosophila* larvae exposed to AgNPs was concurrent with upregulation of p38 MAPK and HSP70 protein.[33] Hence, we anticipated that antioxidant molecules such as the peroxidase enzyme Cat would also be provoked; however, expression of *Cat* was consistently downregulated during 1−6 h exposure. Other antioxidant enzymes metabolizing, for example, superoxide anion would deserve investigation at these time points.

In contrast to THP-1 cells, a gradual increase of the ROS level was recorded in coelomocytes (Figure 3) with concurrent downregulation of *MEKK1*, *HSP70/HSPA8*, and *Cat*. Further, perhaps the most remarkable dissimilarity in coelomocytes was a failure of *MT* induction compared to THP-1 cells. The concentration of AgNPs was not high enough to damage the cell membranes of coelomocytes during 1−6 h exposure, but still the intracellular accumulation of AgNPs (Figure 2) could be enough to locally compromise the early defense system against metal/oxidative stress. Alternatively, the existence of cell populations lacking metallothionein expression[34] could have obscured the overall MT mRNA levels in coelomocytes.

Of particular interest was the late induction of *PKC1/PRKCE* and *MyD88*, presumably being implicated in innate immune functions. The protein kinase C family (encoded by *PKC1/PRKCE*) plays a pivotal role maintaining fundamental cellular functions and homeostasis including immune signaling[35] and phagocytosis of opsonized materials.[36] *MyD88* encodes a central adaptor protein that links Toll-like receptors (TLRs) to downstream signaling of the MAPK pathway and the nuclear transcription factor κB, and integration of those signals leads to inflammation.[37] Stress-activation of MAPKs would interfere with the cross-regulated immune signaling (e.g., TLR-mediated gene programs) and thus modulating cytokine secretion as reported in several studies on AgNPs.[38,39] The crosstalk of stress and immune responses is highly conserved across the animal kingdom. For instance, different types of NPs (Fullerene, TiO_2 and SiO_2) have been reported to affect MAPK signaling events simultaneously altering the immune parameters (e.g., lysozyme release and phagocytosis) in mussel immunocytes.[40]

In summary, conserved molecular signatures probed in this study underpin a potential cascade of early gene responses to AgNPs from oxidative stress to alteration of immune signaling as a shared consequence between coelomocytes and THP-1 cells. An interesting observation was a contrasting regulation of *MT/MT2A* in coelomocytes that accumulated much more AgNPs than THP-1 cells did. As diff.THP-1 cells were more vulnerable than its precursor, the phagocytic population of coelomocytes that are evidently capable of scavenging NPs would likely contribute to the overall toxicity caused by AgNPs.

■ ASSOCIATED CONTENT

Supporting Information

Supplemental experimental methods (preparation of colloidal AgNPs, F-AAS for total silver quantification, endotoxin tests, particle characterization, soluble silver fraction measurements, GFAAS, coelomocyte harvesting, TEM imaging of coelomocytes, RNA extraction, cDNA synthesis, primers and qPCR); gating of coelomocytes in flow cytometry (Figure S1); GenBank accession numbers and primers used for qPCR analysis (Table S1); particle characterization (Figure S2); zeta potential measurements (Figure S3); soluble silver fraction of AgNPs (Figure S4); EC_x values estimated from the cytotoxicity assays (Table S2); Silver accumulation in Ag^+-treated cells (Figure S5); supplemental TEM images and associated EDS profiles of coelomocytes exposed to AgNPs (Figure S6); cell viability following 1−6 h exposure to AgNPs (Figure S7); correspondence analysis of mixed qPCR data set (Figure S8); and temporal gene expression profiles following exposure to AgNPs (Table S3). This material is available free of charge via the Internet at http://pubs.acs.org.

■ AUTHOR INFORMATION

Corresponding Author

*Phone: +45 871 55842; fax: +45 871 55895; e-mail: yuya@inano.au.dk.

Notes

The authors declare no competing financial interest.

■ ACKNOWLEDGMENTS

We gratefully acknowledge Levente László Mácsik for technical assistance during the cytotoxicity assays and the financial support of Aarhus University Research Foundation (AUFF; V-2009-FLS 6-66), the Danish Strategic Research Council (NABIIT 2006-06-0015), the Danish Research Council (FUU 1-5971-10000377) and Medical Faculty Research Foundation, University of Pécs (PTE-ÁOK-KA 34039/10-06).

■ REFERENCES

(1) Benn, T. M.; Westerhoff, P. Nanoparticle silver released into water from commercially available sock fabrics. *Environ. Sci. Technol.* **2008**, *42* (11), 4133−4139.

(2) Kim, B.; Park, C.-S.; Murayama, M.; Hochella, M. F. Discovery and characterization of silver sulfide nanoparticles in final sewage sludge products. *Environ. Sci. Technol.* **2010**, *44* (19), 7509−7514.

(3) Liu, J.; Pennell, K. G.; Hurt, R. H. Kinetics and mechanisms of nanosilver oxysulfidation. *Environ. Sci. Technol.* **2011**, *45* (17), 7345−7353.

(4) Coutris, C.; Hertel-Aas, T.; Lapied, E.; Joner, E. J.; Oughton, D. H. Bioavailability of cobalt and silver nanoparticles to the earthworm *Eisenia fetida*. *Nanotoxicology* **2012**, *6* (2), 186−195.

(5) Heckmann, L.-H.; Hovgaard, M.; Sutherland, D.; Autrup, H.; Besenbacher, F.; Scott-Fordsmand, J. Limit-test toxicity screening of selected inorganic nanoparticles to the earthworm *Eisenia fetida*. *Ecotoxicology* **2011**, *20* (1), 226−233.

(6) Shoults-Wilson, W. A.; Reinsch, B. C.; Tsyusko, O. V.; Bertsch, P. M.; Lowry, G. V.; Unrine, J. M. Effect of silver nanoparticle surface coating on bioaccumulation and reproductive toxicity in earthworms (*Eisenia fetida*). *Nanotoxicology* **2011**, *5* (3), 432−444.

(7) Lapied, E.; Moudilou, E.; Exbrayat, J.-M.; Oughton, D. H.; Joner, E. J. Silver nanoparticle exposure causes apoptotic response in the earthworm *Lumbricus terrestris* (Oligochaeta). *Nanomedicine* **2010**, *5* (6), 975−984.

(8) Shoults-Wilson, W.; Zhurbich, O.; McNear, D.; Tsyusko, O.; Bertsch, P.; Unrine, J. Evidence for avoidance of Ag nanoparticles by earthworms (*Eisenia fetida*). *Ecotoxicology* **2011**, *20* (2), 385−396.

(9) Hartenstein, V. Blood cells and blood cell development in the animal kingdom. *Annu. Rev. Cell Dev. Biol.* **2006**, *22* (1), 677−712.

(10) Cooper, E. L.; Roch, P. Earthworm immunity: A model of immune competence. *Pedobiologia* **2004**, *47*, 676−688.

(11) Stürzenbaum, S. R.; Georgiev, O.; Morgan, A. J.; Kille, P. Cadmium detoxification in earthworms: From genes to cells. *Environ. Sci. Technol.* **2004**, *38* (23), 6283−6289.

(12) Bihari, P.; Vippola, M.; Schultes, S.; Praetner, M.; Khandoga, A.; Reichel, C.; Coester, C.; Tuomi, T.; Rehberg, M.; Krombach, F. Optimized dispersion of nanoparticles for biological in vitro and in vivo studies. *Part. Fibre Toxicol.* **2008**, *5* (1), 14.

(13) Casals, E.; Pfaller, T.; Duschl, A.; Oostingh, G. J.; Puntes, V. Time evolution of the nanoparticle protein corona. *ACS Nano* **2010**, *4* (7), 3623−3632.
(14) Beer, C.; Foldbjerg, R.; Hayashi, Y.; Sutherland, D. S.; Autrup, H. Toxicity of silver nanoparticles—Nanoparticle or silver ion? *Toxicol. Lett.* **2012**, *208* (3), 286−292.
(15) Engelmann, P.; Pálinkás, L.; Cooper, E. L.; Németh, P. Monoclonal antibodies identify four distinct annelid leukocyte markers. *Dev. Comp. Immunol.* **2005**, *29* (7), 599−614.
(16) Park, E.; Jung, H.; Yang, H.; Yoo, M.; Kim, C.; Kim, K. Optimized THP-1 differentiation is required for the detection of responses to weak stimuli. *Inflamm. Res.* **2007**, *56* (1), 45−50.
(17) Foldbjerg, R.; Olesen, P.; Hougaard, M.; Dang, D. A.; Hoffmann, H. J.; Autrup, H. PVP-coated silver nanoparticles and silver ions induce reactive oxygen species, apoptosis and necrosis in THP-1 monocytes. *Toxicol. Lett.* **2009**, *190* (2), 156−162.
(18) Krejsa, C. M.; Schieven, G. L. Detection of oxidative stress in lymphocytes using dichlorodihydrofluorescein diacetate. In *Stress Response*; Walker, J. M., Keyse, S. M., Eds.; Humana Press, 2000; Vol. *99*, pp 35−47.
(19) Peirson, S. N.; Butler, J. N.; Foster, R. G. Experimental validation of novel and conventional approaches to quantitative real-time PCR data analysis. *Nucleic Acids Res.* **2003**, *31* (14), e73.
(20) Heckmann, L.-H.; Sorensen, P.; Krogh, P.; Sorensen, J. NORMA-Gene: A simple and robust method for qPCR normalization based on target gene data. *BMC Bioinf.* **2011**, *12* (1), 250.
(21) Suzuki, H.; Toyooka, T.; Ibuki, Y. Simple and easy method to evaluate uptake potential of nanoparticles in mammalian cells using a flow cytometric light scatter analysis. *Environ. Sci. Technol.* **2007**, *41* (8), 3018−3024.
(22) Lundqvist, M.; Stigler, J.; Elia, G.; Lynch, I.; Cedervall, T.; Dawson, K. A. Nanoparticle size and surface properties determine the protein corona with possible implications for biological impacts. *Proc. Natl. Acad. Sci. U. S. A.* **2008**, *105* (38), 14265−14270.
(23) Walczyk, D.; Bombelli, F. B.; Monopoli, M. P.; Lynch, I.; Dawson, K. A. What the cell "sees" in bionanoscience. *J. Am. Chem. Soc.* **2010**, *132* (16), 5761−5768.
(24) Hollinger, M. A. Toxicological Aspects of Topical Silver Pharmaceuticals. *Crit. Rev. Toxicol.* **1996**, *26* (3), 255−260.
(25) Lunov, O.; Syrovets, T.; Loos, C.; Beil, J.; Delacher, M.; Tron, K.; Nienhaus, G. U.; Musyanovych, A.; Mailänder, V.; Landfester, K.; Simmet, T. Differential uptake of functionalized polystyrene nanoparticles by human macrophages and a monocytic cell line. *ACS Nano* **2011**, *5* (3), 1657−1669.
(26) Limbach, L. K.; Wick, P.; Manser, P.; Grass, R. N.; Bruinink, A.; Stark, W. J. Exposure of Engineered nanoparticles to human lung epithelial cells: influence of chemical composition and catalytic activity on oxidative stress. *Environ. Sci. Technol.* **2007**, *41* (11), 4158−4163.
(27) Navarro, E.; Piccapietra, F.; Wagner, B.; Marconi, F.; Kaegi, R.; Odzak, N.; Sigg, L.; Behra, R. Toxicity of silver nanoparticles to *Chlamydomonas reinhardtii*. *Environ. Sci. Technol.* **2008**, *42* (23), 8959−8964.
(28) Liu, J.; Hurt, R. H. Ion release kinetics and particle persistence in aqueous nano-silver colloids. *Environ. Sci. Technol.* **2010**, *44* (6), 2169−2175.
(29) Locht, L.; Larsen, A.; Stoltenberg, M.; Danscher, G. Cultured macrophages cause dissolucytosis of metallic silver. *Histol. Histopathol.* **2009**, *24*, 167−173.
(30) Reinecke, F.; Levanets, O.; Olivier, Y.; Louw, R.; Semete, B.; Grobler, A.; Hidalgo, J.; Smeitink, J.; Olckers, A.; Van der Westhuizen, F. H. Metallothionein isoform 2A expression is inducible and protects against ROS-mediated cell death in rotenone-treated HeLa cells. *Biochem. J.* **2006**, *395* (2), 405−415.
(31) Eom, H.-J.; Choi, J. p38 MAPK activation, DNA damage, cell cycle arrest and apoptosis as mechanisms of toxicity of silver nanoparticles in jurkat T cells. *Environ. Sci. Technol.* **2010**, *44* (21), 8337−8342.
(32) Hsin, Y. H.; Chen, C. F.; Huang, S.; Shih, T. S.; Lai, P. S.; Chueh, P. J. The apoptotic effect of nanosilver is mediated by a ROS- and JNK-dependent mechanism involving the mitochondrial pathway in NIH3T3 cells. *Toxicol. Lett.* **2008**, *179* (3), 130−139.
(33) Ahamed, M.; Posgai, R.; Gorey, T. J.; Nielsen, M.; Hussain, S. M.; Rowe, J. J. Silver nanoparticles induced heat shock protein 70, oxidative stress and apoptosis in *Drosophila melanogaster*. *Toxicol. Appl. Pharmacol.* **2010**, *242* (3), 263−269.
(34) Olchawa, E.; Bzowska, M.; Stürzenbaum, S. R.; Morgan, A. J.; Plytycz, B. Heavy metals affect the coelomocyte-bacteria balance in earthworms: Environmental interactions between abiotic and biotic stressors. *Environ. Pollut.* **2006**, *142* (2), 373−381.
(35) Aksoy, E.; Goldman, M.; Willems, F. Protein kinase C epsilon: A new target to control inflammation and immune-mediated disorders. *Int. J. Biochem. Cell Biol.* **2004**, *36* (2), 183−188.
(36) Larsen, E. C.; Ueyama, T.; Brannock, P. M.; Shirai, Y.; Saito, N.; Larsson, C.; Loegering, D.; Weber, P. B.; Lennartz, M. R. A role for PKC-ε in FcγR-mediated phagocytosis by RAW 264.7 cells. *J. Cell Biol.* **2002**, *159* (6), 939−944.
(37) Wong, C. K.; Li, P. W.; Lam, C. W. K. Intracellular JNK, p38 MAPK and NF-κB regulate IL-25 induced release of cytokines and chemokines from costimulated T helper lymphocytes. *Immunol. Lett.* **2007**, *112* (2), 82−91.
(38) Shin, S. H.; Ye, M. K.; Kim, H. S.; Kang, H. S. The effects of nano-silver on the proliferation and cytokine expression by peripheral blood mononuclear cells. *Int. Immunopharmacol.* **2007**, *7* (13), 1813−1818.
(39) Castillo, P. M.; Herrera, J. L.; Fernandez-Montesinos, R.; Caro, C.; Zaderenko, A. P.; Mejías, J. A.; Pozo, D. Tiopronin monolayer-protected silver nanoparticles modulate IL-6 secretion mediated by Toll-like receptor ligands. *Nanomedicine* **2008**, *3* (5), 627−635.
(40) Canesi, L.; Ciacci, C.; Vallotto, D.; Gallo, G.; Marcomini, A.; Pojana, G. In vitro effects of suspensions of selected nanoparticles (C60 fullerene, TiO_2, SiO_2) on *Mytilus* hemocytes. *Aquat. Toxicol.* **2010**, *96* (2), 151−158.